Check for updates

Fucosterol's modulatory effects on interleukin-6 and interleukin-1β: insights from molecular docking and lipopolysaccharide-induced HEK293 cells and zebrafish embryos

Rickson Gaspe[1], Junie Billones[2], Agnes Llamasares-Castillo[1, 3, 4, *]

[1] Pharmacy Cluster, The Graduate School, University of Santo Tomas, Manila 1008, Philippines
[2] Department of Physical Sciences & Mathematics, University of the Philippines–Manila, Manila 1000, Philippines
[3] Research Center for the Natural & Applied Sciences, University of Santo Tomas, Manila 1008, Philippines
[4] Department of Pharmacy, Faculty of Pharmacy, University of Santo Tomas, Manila 1008, Philippines

Abstract

Chronic inflammatory diseases remain among the leading causes of death worldwide, highlighting the need for safer and more cost-effective anti-inflammatory agents from natural resources. Fucosterol, a bioactive compound isolated from brown marine algae, has been reported to exhibit various pharmacological properties, including anti-inflammatory activity. However, further investigation is needed to elucidate its mechanisms of action. This study assessed the anti-inflammatory potential of fucosterol using *in silico*, *in vitro*, and *in vivo* approaches. Reverse molecular docking revealed strong binding affinities with interleukin (IL)-6 (–6.3 kcal/mol) and IL-1β (–7.4 kcal/mol), suggesting potential interactions with key inflammatory cytokines. Moreover, absorption, distribution, metabolism, excretion, and toxicity (ADMET) profiling highlighted fucosterol's favorable drug-likeness and toxicity profile. Toxicity assessments, including the MTT assay on Human Embryonic Kidney (HEK293) cells and the zebrafish embryo acute toxicity assay, showed concentration-dependent effects, with half-maximal inhibitory concentration (IC_{50}) and medial lethal concentration (LC_{50}) values of 279.90 μg/mL and 173.60 μg/mL, respectively. *In vitro* Enzyme-Linked Immunosorbent Assay (ELISA)-based assay using lipopolysaccharide-induced HEK293 cells demonstrated a biphasic response in inhibiting IL-6 (24 and 48 h IC_{50} = 5.86 and 73.36 μg/mL) and IL-1β (24 and 48 h IC_{50} = 2.59 and 0.02 μg/mL). Similarly, *in vivo* analysis using lipopolysaccharide-induced zebrafish embryos showed a significant reduction in IL-6 (24 and 48 h IC_{50} = 34.54 and 30.28 μg/mL) and IL-1β (24 and 48 h IC_{50} = 29.39 and 29.61 μg/mL) at higher concentrations. These findings provide valuable insights into fucosterol's role in modulating inflammatory cytokines, likely through the NF-κB pathway. The study provides a better understanding of fucosterol's anti-inflammatory mechanisms, supporting its potential for further pharmacological research. Future studies, including clinical validation and mechanistic studies, are necessary to establish its therapeutic use and application.

Keywords: Seaweed, Algae, Inflammation, Cytokines, Zebrafish

Introduction

Chronic inflammatory diseases, including neoplasms, cerebro-vascular diseases, and hypertension, remain the leading causes of mortality in the Philippines (Ornos et al., 2023). Inflammation, the body's natural defense mechanism, facilitates the removal of harmful pathogens and stimulants but can become detrimental when transitioning from an acute to a chronic state. Chronic inflammation is driven by prolonged exposure to inflammatory stimuli, leading to tissue degeneration and the onset of diseases such as asthma, cancer, diabetes, and osteoarthritis (Chen et al., 2018 ; Franceschi et al., 2014; Germolec et al., 2018). With this, continuous efforts to generate knowledge on the role of inflammation in chronic diseases and develop effective treatment strategies in combatting inflammation are critical to mitigating this problem (Ornos et al., 2023; PSA, 2023).

Complex pathways mediate inflammatory processes, primarily involving the release of cytokines like interleukins (ILs), chemokines, interferons (IFNs), and tumor necrosis factors (TNFs), which modulate immune responses by either promoting or inhibiting inflammation (Chen et al., 2018; Turner et al., 2014). Pharmacological interventions, including monoclonal antibodies (MABs) and non-steroidal anti-inflammatory drugs (NSAIDs), have been developed to modulate these pathways and control inflammation (Gerriets et al., 2023). However, NSAIDs are associated with gastrointestinal toxicity and cardiovascular risks, while MABs can lead to immunosuppression and hypersensitivity reactions (Pirlamarla & Bond, 2016; Yatoo et al., 2018). These adverse effects underscore the need for safer and more effective alternatives derived from natural products.

One promising natural product is fucosterol (Fig. 1), a bioactive sterol derived from brown seaweed, which has demonstrated significant pharmacological properties, including anti-inflammatory, antioxidant, neuroprotective, and anticancer effects (Jang et al., 2024; Meinita et al., 2021). Moreover, fucosterol has also shown favorable toxicity profiles in cell viability assays, making it a strong candidate for drug development (Meinita et al., 2021). Thus, further evaluation of its pharmacological activities is crucial in establishing the compound's potential as a pharmaceutical agent.

Recent advancements in drug discovery have facilitated the study of plant-derived compounds using molecular docking and computational modeling, which predict interactions between a compound and target proteins (Kazmi et al., 2019; Meng et al., 2011). While these in silico methods enhance drug discovery efficiency, their findings must be validated through in vitro and in vivo studies to confirm bioactivity. Experimental models, such as the lipopolysaccharide (LPS)-induced inflammation model in Human Embryonic Kidney (HEK293) cells, provide controlled environments to assess fucosterol's effects on cytokine expression in non-immune cells, while zebrafish models allow for the study of inflammation in physiologically relevant systems (Novoa & Figueras, 2011; Raghubeer et al., 2017; Tan et al., 2021). These approaches provide crucial insights into the pharmacological mechanisms of fucosterol and support its potential development as a safer alternative to synthetic anti-inflammatory drugs.

This study provides relevant insights to establish further fucosterol's potential in regulating inflammatory cytokines and chronic inflammation. By providing comprehensive insights into its anti-inflammatory activity, this research contributes to developing natural product-derived pharmaceutical products that may effectively manage chronic inflammatory diseases. Furthermore, it aligns with broader efforts to explore natural product-based therapeutics, reinforcing the importance of alternative anti-inflammatory agents in modern medicine.
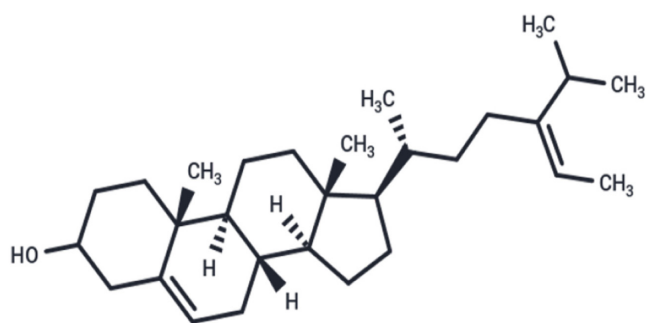
Materials and Methods

Fucosterol source
Fucosterol | Cat.No. T8184 (TargetMol Chemicals, Boston, MA, USA).

Reverse molecular docking and ADMET profiling studies
All *in silico* molecular docking simulations were performed based on previously reported methodologies and using the computers and software in the laboratory of the emerging inter-

Fig. 1. Structure of fucosterol (TargetMol chemicals).

disciplinary research (EIDR) program of the University of the Philippines–Manila, Philippines (Agu et al., 2023; Alos et al., 2020; Aventurado et al., 2020; Bell & Zhang, 2019).

Ligand and protein preparation

The molecular structures of fucosterol, known inhibitors, and the target pro-inflammatory proteins were downloaded from the PubChem (https://pubchem.ncbi.nlm.nih.gov/) and RCSB (https://www.rcsb.org/) online databases, respectively. Using Spartan '14 (1.1.4), the structures of the ligands were optimized through the computation feature's molecular mechanics and converted to appropriate formats to allow loading in other programs. The structure of the pro-inflammatory proteins was prepared through BIOVIA discovery studio (DS) visualizer (17.2.0.16349, Bio-Techne, Minneapolis, MN, USA) by the removal of the attached heteroatoms or ligands and the addition of polar hydrogen atoms to allow and give space for the docking of new ligands. The following pro-inflammatory proteins were selected for this study: Interleukin-1 Beta (IL-1β, PDB ID: 8C3U), Thromboxane A2 (TXA2, PDB ID: 6IIV), Interleukin-6 (IL-6, PDB ID: 1ALU), Cyclooxygenase-2 (COX-2, PDB ID: 5KIR), Transforming Growth Factor Beta (TGF-β, PDB ID: 1PY5), and Lipoxygenase-3 (LOX-3, PDB ID: 1NO3).

Docking simulation

To assess fucosterol's binding energies with the target pro-inflammatory proteins, docking simulations were performed using PyRx–Python Prescription (0.9.8). The docking protocol was validated using an online tool called DockRMSD, developed by the University of Michigan's Zhong Laboratories, to compute the root mean square deviation (RMSD) values (Bell & Zhang, 2019). Furthermore, Chimera (1.12) was used to visualize the structures of the original and redocked ligands for further validation. All ligands were docked onto the optimized grid-box dimension for four cycles with the following settings: exhaustiveness = 8 and max number of modes = 9, generating 36 poses per protein-ligand complex. BIOVIA DS was utilized to visualize and enlist the key interacting amino acid residues and evaluate their molecular interactions.

ADMET profiling

To predict the drug-likeness profile of fucosterol, including its absorption, distribution, metabolism, and excretion (ADME) properties, SwissADME (http://www.swissadme.ch/) was used. Moreover, pharmacokinetic properties like gastrointestinal absorption and blood-brain barrier permeability were also predicted using the Brain or IntestinaL EstimateD permeation (BOILED-Egg) model in SwissADME. To evaluate fucosterol's predicted toxicity profile, BIOVIA DS's Toxicity Prediction by Komputer Assisted Technology (TOPKAT) tool and Prediction of Toxicity of Chemicals (ProTox) Version 3 (https://tox.charite.de/protox3/) were used.

MTT assay

HEK293 cell lines were procured from the Mammalian Tissue Culture Laboratory of the University of Santo Tomas–Research Center for the Natural and Applied Sciences (UST–RCNAS), Manila, Philippines. Cells were grown and cultured following standard procedures based on previous literature (Erukainure et al., 2018; Javadi et al., 2020). The cells were incubated with various concentrations of fucosterol (0.1–2,000 μg/mL), and separate wells were assigned with 20 μg/mL Paclitaxel (positive control). Standard MTT assay procedures were performed based on the study of Yoojam et al. (2021), where the cell viability was evaluated using the absorbances from the readings under the wavelength of 570nm using a microplate reader (Yoojam et al., 2021). HEK293 cells and the positive control paclitaxel were selected for this study based on the works of previously published articles (Raghubeer et al., 2017; Yadav et al., 2020).

In Vitro determination of IL-6 and IL-β expression

Based on the results of the MTT assay, five concentrations of Fucosterol (0.1 μg/mL to 62.50 μg/mL) and the control drug 5 μg/mL dexamethasone (DEX) were added to a 24-well plate containing the pre-seeded HEK293 cell lines (1.5 × 105 cells/mL). Inflammation was induced by administering 1 μg/mL of LPS from *Escherichia coli* to the wells containing the cells incubated with Fucosterol after 1 hour. After 24 and 48 h, the supernatants from each well were collected and transferred to individual tubes for further assays (Bin et al., 2023; Sun et al., 2015; Yoojam et al., 2021). Using the instructions provided by the manufacturer of uncoated Enzyme-Linked Immunosorbent Assay (ELISA) kits for IL-6 | Cat. No. 430504 and IL-1β | Cat. No. 437004 (Biolegend, San Diego, CA, USA), the expression level of IL-6 and IL-1β in the supernatant fluid was measured. GraphPad Prism (10.4.1) was used to calculate the half-maximal inhibitory concentration (IC_{50}) by plotting the dose-response curve using non-linear regression analysis (Aykul & Martinez-Hackert, 2016; Nadri et al., 2014).

Zebrafish embryo acute toxicity assay

Adult zebrafish were purchased from a local market located in Cartimar, Pasay City, Philippines. The zebrafish were allowed to acclimatize in the Pharmacology Laboratory of the UST-RC-NAS following the conditions stated in the Organization for Economic Cooperation and Development (OECD) guidelines (OECD, 2013; Wang et al., 2021). Following the OECD's acute toxicity testing guidelines (Test 236), the fish embryo acute toxicity (FET) test for fucosterol was done for 96 h. Two trials were performed, and observations were made every 24 h for the following apical parameters: coagulated embryos, lack of somite formation, non-detachment of the tail, and lack of heartbeat (OECD, 2013). Using the data from the observations, the medial lethal concentration (LC_{50}) was computed using non-linear regression analysis in GraphPad Prism.

In Vivo determination of IL-6 and IL- β expression

Similarly, five concentrations of fucosterol (6.25 μg/mL to 100 μg/mL) and the control drug 5 μg/mL DEX were administered to each well containing the embryos. After an hour, they were treated with 10 μg/mL LPS to induce inflammation. After 24 and 48 h, the embryos were transferred to individual tubes, homogenized using cold saline, and centrifuged at 5,000 repetitions per minute (rpm) for 10 min at 4℃. The supernatants were collected from each tube and were kept for further analysis (Wang et al., 2021, 2022; Yang et al., 2014). Expression of IL-6 and IL-1β in the supernatants was determined by following the manufacturer's instructions using pre-coated ELISA kits for IL-6 | ELK9663 and IL-1β | ELK8505 (ELK Biotechnology, Wuhan, China) where the percentage inhibition at 450nm was used to determine the IC_{50} through non-linear regression analysis in GraphPad Prism.
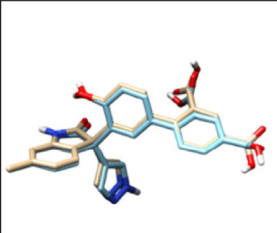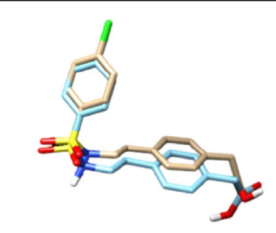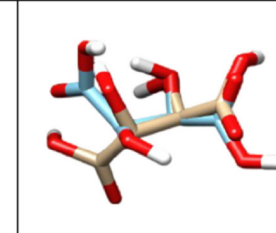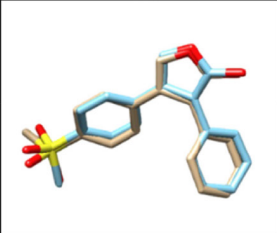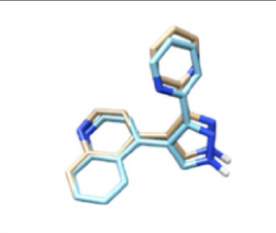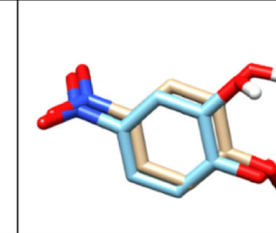
Statistical treatment

All tests were conducted in triplicates and were tested for significant differences using one-way ANOVA and Post Hoc Tukey's test ($p \leq 0.05$) using Microsoft Excel (Redmond , WA, USA), the Statistical Package for the Social Sciences (SPSS, Chicago, IL, USA), and RStudios (Posit, Boston, MA, USA).

Results and Discussion

Reverse molecular docking simulation with selected pro-inflammatory proteins

Docking simulations were performed to determine the accuracy of the redocking process of the originally bound ligands to their respective target proteins where RMSD values ranged from 0.465 to 1.968 Å, which are within the acceptable range

IL-1β (T9C)	TXA2 (Daltroban)	IL-6 (Tartaric Acid)
PDB ID: 8C3U	PDB ID: 6IIV	PDB ID: 1ALU
RMSD: 0.714 Å	RMSD: 0.907 Å	RMSD: 1.968 Å
COX-2 (Rofecoxib)	TGF-β (PY1)	LOX-3 (4-Nitrocatechol)
PDB ID: 5KIR	PDB ID: 1PY5	PDB ID: 1NO3
RMSD: 0.865 Å	RMSD: 1.183 Å	RMSD: 0.465 Å

Fig. 2. RMSD values of the superimposed structures of the original bound (light blue) and redocked (beige) ligands of the pro-inflammatory proteins. COX, cyclooxygenase; IL, interleukin; LOX, lipoxygenase; PDB, protein data bank; RMSD, root mean square deviation; TGF, transforming growth factor; TXA, thromboxane.

of 0 to 2.0 Å (Fig. 2; Agu et al., 2023). The proteins' active sites were defined using the optimized grid-box dimensions, which guided the docking of fucosterol and known inhibitors (Table 1).

The binding mode with the most negative binding energy among the several cycles was selected as the most favorable docking pose and was included in the analysis. Fucosterol exhibited negative binding energies with all proteins, indicating its ability to form stable complexes with the targets. Notably,

fucosterol's lowest binding energies were reported with IL-1β, TXA2, and IL-6, at –7.4 kcal/mol, –6.7 kcal/mol, and -6.3 kcal/mol, respectively (Table 2). However, fucosterol showed more negative binding energy with IL-6 and IL-1β when compared with the known inhibitors' results. These suggest that fucosterol can effectively bind and inhibit the progression of these proteins, potentially delaying the progression of chronic inflammatory diseases mediated by these targets. The anti-inflammatory

Table 1. Optimized grid box dimensions of the pro-inflammatory proteins

Pro-Inflammatory Protein	PDB ID	Resolution (Å)	Descriptive Title	Grid Box Parameters
Interleukin-1 Beta (IL-1β)	8C3U	1.95	Crystal Structure of human IL-1beta in complex with a low molecular weight antagonist	Center: x = –19.441, y = –3.971, z = –52.623 Dimensions (Å): x = 24.006, y = 26.510, z = 33.370
Thromboxane A2 (TXA2)	6IIV	3.0	Crystal structure of the human thromboxane A2 receptor bound to Daltroban	Center: x = 22.809, y = 162.113, z = 144.106 Dimensions (Å): x = 24.377, y = 24.354, z = 20.799
Interleukin-6 (IL-6)	1ALU	1.90	Human Interleukin-6	Center: x = –8.024, y = –12.226, z = 2.518 Dimensions (Å): x = 12.545, y = 14.571, z = 9.935
Cycloxygenase-2 (COX-2)	5KIR	2.7	The Structure of Vioxx Bound to Human COX-2	Center: x = 23.185, y = –0.532, z = 35.718 Dimensions (Å): x = 18.484, y = 21.137, z = 19.336
Transforming Growth Factor-Beta (TGF-β)	1PY5	2.30	Crystal Structure of TGF-beta receptor I kinase with inhibitor	Center: x = 3.416, y = 10.764, z = 4.758 Dimensions (Å): x = 7.646, y = 10.907, z = 9.019
Lipoxygenase-3 (LOX-3)	1NO3	2.15	Refined Structure of Soybean Lipoxygenase-3 with 4-Nitrocatechol at 2.5 Angstrom Resolution	Center: x = 20.001, y = 6.214, z = 17.866 Dimensions (Å): x = 16.731, y = 15.514, z = 19.137

COX, cyclooxygenase; IL, interleukin; LOX, lipoxygenase; PDB, protein data bank; TGF, transforming growth factor; TXA, thromboxane.

Table 2. Fucosterol and known inhibitors binding energies and key interacting amino acid residues with selected pro-inflammatory proteins

Inflammatory proteins/ PDB ID	Ligands	Binding Energy (kcal/mol)	Key interacting amino acid residues
IL-1β (8C3U)	Test compound: fucosterol	–7.4	VAL3, PHE46, VASL47, LYS55 PRO57, VAL58, ALA59, MET95, LYS92, LYS93, LYS94, LYS97, VAL100, ASN102, ALA115, PRO118
	Known inhibitor: anakinra	–6.2	VAL3, ARG4, SER5, LEU6, ASN7, VAL41, PHE42, SER43, SER45, LEU62, LYS63, GLU64, LYS65, PRO91, SER152
	Known inhibitor: ustekinumab	–6.7	ALA1, VAL3, SER45, PHE46, VAL47, GLU50, PRO57, VAL58, ALA59, PRO91, LYS92, LYS93, LYS94, MET95, VAL100
	Co-crystallized ligand: T9C	–10.0	VAL3, SER45, PHE46, VAL47, GLU50, LYS55, PRO57, VAL58, ALA59, PRO91, LYS92, LYS93, LYS94, MET95, LYS97, VAL100, ASN102, ALA115
TXA2 (6IIV)	Test compound: fucosterol	–6.7	PHE30, ALA31, PHE34, CYS35, GLY77, LEU78, THR81, GLY82, VAL85, VAL86, HIS89, MET112, PHE115, GLY116, TRP258, LEU294, ARG295, THR298, GLN301
	Known inhibitor: BM-573	–8.8	PHE30, PHE34, CYS35, GLY77, LEU78, THR81, GLY82, VAL85, MET108, MET112, PHE115, SER181, TRP182, LEU291, LEU294, ARG295, THR298, TRP299, GLN301,

Table 2. Continued

| Inflammatory proteins/ PDB ID	Ligands	Binding Energy (kcal/mol)	Key interacting amino acid residues
TXA2 (6IIV)	Known inhibitor: picotamide	−9.7	PHE30, ALA31, PHE34, LEU78, THR81, VAL85, MET108, MET112, PHE115, GLY116, SER181, TRP182, TRP258, LEU291, LEU294, ARG295, ALA297, THR298, ALA299, GLN301
	Known inhibitor: terutroban	−11.2	PHE30, ALA31, PHE34, CYS35, GLY77, LEU78, THR81, GLY82, VAL85, MET112, PHE115, GLY116, PRO179, SER181, TRP182, PHE184, PHE200, TRP258, LEU291, LEU294, ARG295, ALA297, THR298
	Co-crystallized ligand: daltroban	−9.2	ALA31, GLY77, LEU78, THR81, VAL85, HIS89, MET112, PHE115, GLY116, PRO179, SER181, PHE184, PHE200, TRP258, LEU291, LEU294, ARG295, ALA297, THR298, GLN301
IL-6 (1ALU)	Test compound: fucosterol	−6.3	LYS66, MET67, PHE74, GLN75, SER76, GLU172, SER176, ARG179
	Known inhibitor: methotrexate	−4.0	ASP26, ARG30, LEU33, GLN175, SER176, LEU178, ARG179, ARG182
	Known inhibitor: oxaprozin	−5.5	ARG30, LEU33, GLN175, SER176, LEU178, ARG179, ARG182
	Co-crystallized ligand: tartaric acid	−3.8	GLN175, SER176, LEU178, ARG179, ARG182
COX-2 (5KIR)	Test compound: fucosterol	−4.6	VAL89, LEU93, VAL116, ARG120, VAL349, LEU352, SER353, TYR355, PHE357, LEU359, PHE381, LEU384, TYR385, TRP387, PHE518, MET522, VAL523, GLY526, ALA527, SER530, LEU531
	Known inhibitor: celecoxib	−11.5	HIS90, THR94, VAL116, ARG120, GLN192, VAL349, LEU352, SER353, GLY354, TYR355, LEU359, LEU384, TRP387, ARG513, ALA516, ILE517, PHE518, MET522, VAL523, GLY526, ALA527, SER530, LEU531,
	Known inhibitor: aspirin	−6.5	TYR348, VAL349, LEU352, SER353, PHE381, LEU384, TYR385, TRP387, PHE528, MET522, VAL523, GLY526, ALA527, SER530, LEU531
	Known inhibitor: isoxicam	−7.2	GLN192, GLU346, ASP347, ASN350, HIS351, GLY354, SER579, PHE580, SER581,
	Known inhibitor: ketorolac	−8.8	VAL116, ARG120, VAL349, LEU352, SER353, TYR355, LEU359, PHE381, TRP387, PHE518, MET522, VAL523, GLY526, ALA527, SER530, LEU531
	Co-crystallized ligand: rofecoxib	−10.1	HIS90, GLN192, LEU351, SER353, VAL349, LEU352, TYR355, TRP387, ARG513, ALA516, ILE517, PHE518, MET522, VAL523, GLY526, ALA527, SER530
TGF-β (1PY5)	Test compound: fucosterol	−3.4	ILE211, GLY212, VAL219, ALA230, VAL231, LYS232, PHE234, GLU245, LEU260, LEU278, SER280, ASP281, TYR282, HIS283, GLU284, GLY286, SER287, LYS337, LEU340
	Known inhibitor: tranilast	−7.1	ILE211, GLY212, LYS213, GLY214, VAL219, ALA230, LYS232, LEU260, SER280, ASP281, TYR282, HIS283, GLY286, SER287, LYS337, LEU340, ALA350, ASP351
	Known inhibitor: imatinib mesylate	−3.1	VAL219, LYS232, GLU245, LEU260, LEU340, ALA350, ASP351, LEU352
	Known inhibitor: MG-132	0.9	ILE211, GLY212, LYS213, GLY214, VAL219, ALA230, VAL231, LYS232, TYR249, SER280, ASP281, TYR282, GLY286, ALA350, LEU260, HIS283, SER287, LYS337, LEU340, ASP351
	Co-crystallized ligand: PY1	−7.2	ILE211, VAL219, ALA230, VAL231, LYS232, LEU260, LEU278, SER280, ASP281, TYR282, HIS283, GLY286, LEU340, ASP351
LOX-3 (1NO3)	Test compound: fucosterol	−3.1	THR274, LEU277, GLN514, HIS518, TRP519, HIS523, ILE557, LEU560, ALA561, LEU565, VAL571, ILE572, TYR575, PHE576, GLN716, ILE765, ASP766, VAL769, ILE770, LEU773, ILE857,
	Known inhibitor: zileuton	−2.6	GLN514, HIS518, TRP519, HIS523, ILE557, ALA561, LEU565, VAL571, ILE572, THR575, PHE576, GLN716, ASP766, VAL769, ILE770, LEU773, ILE857

Table 2. Continued

Inflammatory proteins/ PDB ID	Ligands	Binding Energy (kcal/mol)	Key interacting amino acid residues
LOX-3 (1NO3)	Known inhibitor: REV-5901	0.1	LEU277, GLN514, LEU515, HIS518, TRP519, HIS523, ILE557, ALA561, LEU565, VAL566, VAL571, ILE572, THR575, PHE576, ILE765, ASP766, VAL769, ILE770, LEU773, ILE857,
	Co-crystallized ligand: 4-Nitrocatechol	−4.9	LEU277, GLN514, HIS518, TRP519, HIS523, ILE557, ASN558, ALA561, LEU565, VAL566, ILE572, LEU773, ILE857

COX, cyclooxygenase; IL, interleukin; LOX, lipoxygenase; PDB, protein data bank; TGF, transforming growth factor; TXA, thromboxane.

activity of fucosterol was evaluated through both *in vitro* and *in vivo* assays by quantifying the expression levels of IL-6 and IL-1β, which were selected based on the findings from *in silico* studies.

For IL-6, residues including GLN175, SER176, LEU178, and ARG179 were found to be commonly interacting with the
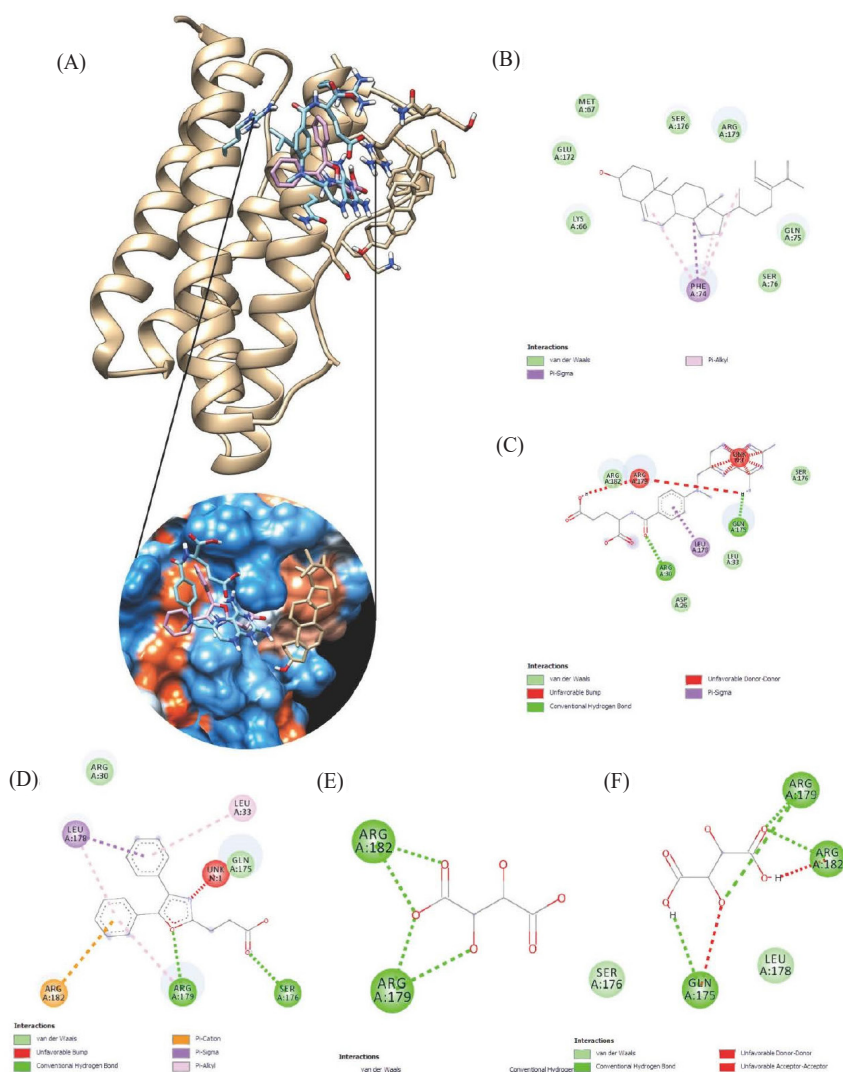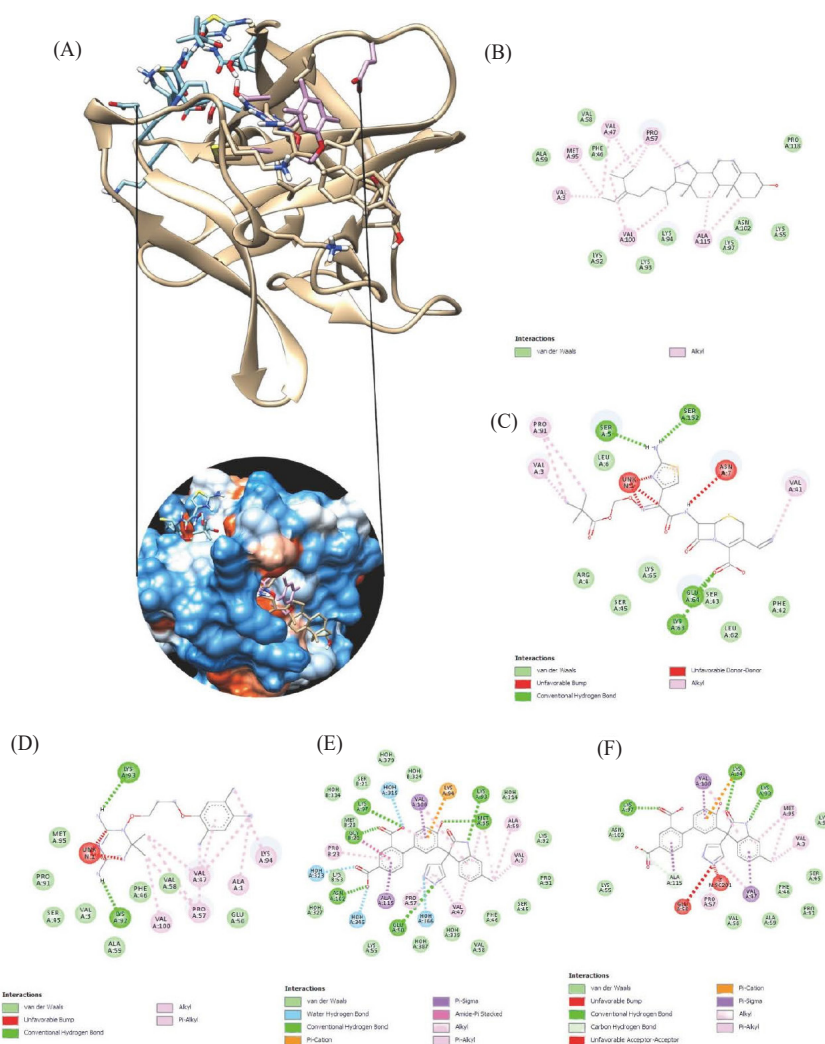

Fig. 3. 3D and 2D Interactions of Fucosterol with Interleukin-6. (A) superimposition of the docked fucosterol (brown) and standard inhibitors methotrexate (blue) and oxaprozin (purple) in IL-6 active site. 2D interactions of (B) fucosterol, (C) methotrexate, (D) oxaprozin, (E) originally-bound tartaric acid, and (F) redocked tartaric acid in IL-6 active site. IL, interleukin.

various ligands (Fig. 3). Moreover, the overlay of fucosterol with methotrexate and oxaprozin helps visualize how fucosterol fits within the binding pocket in comparison to known inhibitors. Since fucosterol aligns well with these inhibitors, it suggests that it could exhibit comparable inhibitory effects on IL-6.

The interaction with SER176 and ARG179 involves hydrogen binding, enhancing binding affinity and stability, while LEU178 contributes to hydrophobic interactions, further strengthening ligand engagement. These interactions strengthen ligand affinity and prevent dissociation, which is essential for prolonged inhibition of the cytokine; thus, these residues play vital roles in stabilizing ligand binding, contributing to the inhibition of the IL-6 signaling pathway (Tran et al., 2022).

Fucosterol's binding with IL-6 involved residue interactions with PHE74, GLN175, SER176, and ARG179. PHE74 facilitates pi-stacking interactions, which occur when aromatic rings interact with other rings or electron-rich systems, stabilizing the ligand within the binding site. In addition, GLN175 influences IL-6's conformational dynamics, potentially interfering with its signaling pathway by inducing structural shifts in IL-6. Moreover, SER176 and ARG179 provide electrostatic stability, aiding in the prolonged inhibition of IL-6 expression (Tran et al., 2022). These interactions suggest that fucosterol can effectively regulate inflammation by modulating IL-6 signaling pathways, crucial in controlling chronic inflammatory diseases like rheumatoid arthritis (Gabay, 2006; Rahman et al., 2021).

Fig. 4. 3D and 2D Interactions of Fucosterol with Interleukin-1β. (A) superimposition of the docked fucosterol (brown) and standard inhibitors anakinra (blue) and ustekinumab (purple) in IL-1β active site. 2D interactions of (B) fucosterol, (C) anakinra, (D) ustekinumab, (E) originally-bound T9C, and (F) redocked T9C in IL-1β active site. IL, interleukin.

For IL-1β, fucosterol's residues are primarily reported through hydrophobic interactions with VAL3, PHE46, VAL47, ALA59, and VAL100 (Fig. 4). These nonpolar residues contributed to hydrophobic forces, which lead to ligand stabilization, thus, reducing IL-1β activity through the alteration of the binding of receptors or signaling proteins.

Like in IL-6, fucosterol occupies a similar binding region as anakinra or ustekinumab, suggesting potential inhibitory effects on IL-1β. Since anakinra primarily inhibits IL-1β by blocking the receptor interaction and ustekinumab downregulating interleukin's signaling pathway, this suggests that fucosterol affects inflammatory pathways through direct hydrophobic engagement. Thus, by creating a hydrophobic environment that stabilizes the ligand-binding site, IL-1β activity is inhibited. Moreover, hydrophobic interactions like these are critical in reducing the production of similar inflammatory cytokines like IL-6 and TNF-α, thus managing inflammatory response (Abdul et al., 2016; Mo et al., 2018).

Overall, the docking simulations underscore the therapeutic potential of fucosterol in the modulation of key inflammatory pathways through cytokine inhibition. The interactions of fucosterol with critical residues in IL-6 and IL-1β provide insight into its mechanism of action, emphasizing its role in managing chronic inflammatory diseases, which needs to be further validated by performing succeeding assays on cellular or animal models. The selected proteins for molecular docking were chosen based on their vital roles in the development and progression of major chronic inflammatory diseases like diabetes and cancer. Their roles in sustaining prolonged inflammatory signaling make them relevant targets for assessing the potential anti-inflammatory activity of natural compounds. This selection is well-supported by existing literature emphasizing their importance as biomarkers and therapeutic targets in chronic inflammation-related research (Chen et al., 2018; Turner et al., 2014).

ADMET profiling

Fucosterol's physicochemical and pharmacokinetic properties were also predicted and evaluated, focusing on its gastrointestinal absorption potential and ability to cross the blood-brain barrier (BBB). Results show that fucosterol exhibits poor pharmacokinetic properties, including low GI absorption due to its poor water solubility profile. Moreover, fucosterol also exhibits poor BBB permeability due to its lipophilicity profile, which is favorable, especially for drugs that are not meant to enter the

Table 3. Summarized ADME properties based on SwissADME and BOILED-egg model

Lipinski's rule of five		
Parameter	Acceptable range	Result
Molecular Weight (g/mol)	≤ 500	412.69 g/mol
Lipophilicity (MLogP)	≤ 4.15	6.62
Hydrogen bond donors (NH/OH)	≤ 5	1
Hydrogen bond acceptors (N/O)	≤ 10	1
Rule violation	≤ 1	1
Molecular drug-likeness	Yes, 1 violation	
BOILED-egg predictions		
Parameter		Result
Passive absorption in the GI tract		No
BBB permeant		No
Lipinski's rule of five		
Parameter	Acceptable range	Result
Molecular weight (g/mol)	≤ 500	412.69 g/mol
Lipophilicity (MLogP)	≤ 4.15	6.62
Hydrogen bond donors (NH/OH)	≤ 5	1
Hydrogen bond acceptors (N/O)	≤ 10	1
Rule violation	≤ 1	1
Molecular drug-likeness	Yes, 1 violation	
BOILED-egg predictions		Result
Passive absorption in the GI tract		No
BBB permeant		No

ADME, absorption, distribution, metabolism, and excretion; BBB, blood-brain barrier; BOILED-egg, brain or Intestinal estimated permeation; GI, gastrointestinal.

brain and exhibit neurological effects (Table 3). Nevertheless, fucosterol satisfied Lipinski's Rule of Five with only one viola-

Table 4. Fucosterol's toxicity profile prediction on animal models using TOPKAT tool

Parameter	Fucosterol
Female rat carcinogen	Single-Carcinogen
Male rat carcinogen	Non-Carcinogen
Ames prediction	Non-mutagen
Skin irritancy	Moderate
Skin sensitization	Weak
Ocular irritancy	Non-Irritant
Rat oral LD$_{50}$	1.92 g/kg body weight
Rat maximum dose feed	0.03 g/kg body weight
Rat maximum dose gavage	0.14 g/kg body weight
Rat inhalational LC$_{50}$	6,057.88 mg/m^3/h

LD$_{50}$, median lethal dose; LC$_{50}$, medial lethal concentration; TOPKAT, Toxicity Prediction by Komputer Assisted Technology.

tion (MLogP > 4.15), indicating its potential utility as a pharmaceutical agent through its favorable drug-likeness profile.

Toxicity profiling provided further insights into fucosterol's safety profile (Table 4). Fucosterol was predicted to be a single-carcinogen in female rats but a non-carcinogen in males. This sex-specific carcinogenic effect warrants further investigation into underlying hormonal or metabolic pathway differences between sexes to establish fucosterol's carcinogenic potential further. Moreover, fucosterol was determined to be a non-mutagenic, moderately skin irritant, weak sensitizer, and non-irritant for ocular applications, making it suitable for use in pharmaceutical formulations like cosmetics. Fucosterol also showed moderate toxicity through a predicted oral LD_{50} of 1.92 g/kg body weight and high inhalational LC_{50} (6,057.88 mg/m^3/h), which suggests safety for oral and inhalational delivery methods.

Oral toxicity predictions also revealed that fucosterol is classified under Class 4, which generally corresponds to compounds with low to moderate toxicity. In addition, fucosterol was also evaluated for organ toxicity, where it was found to have no hepatotoxic, carcinogenic, mutagenic, or cytotoxic effects; however, it may have immunotoxic effects, meaning it could impact immune function by immunosuppression or immunostimulation (Table 5).

Fucosterol's ADMET profile predictions highlight the compound's potential in therapeutic contexts and should not limit the clinical applicability of the compound. Thus, further studies are needed to elucidate and reinforce its pharmacological use.

MTT assay of fucosterol on HEK293 cell lines

Fucosterol's effect on the cell viability of HEK293 cells was evaluated at concentrations from 0.1 to 2,000 µg/mL. Paclitaxel was used as a positive control due to its well-established cytotoxic activity, allowing the benchmarking of cell viability responses (Yadav et al., 2020). Results revealed that concentrations above 62.50 µg/mL were toxic to the cells, where lower concentrations exhibited ≥ 80% viability, indicating low toxicity and promotion of cell viability. Fig. 5 shows the IC_{50} value, which was determined to be 279.90 µg/mL, where a concentration-dependent decrease in cell viability was found to be statistically significant ($p \leq 0.01$).

Similar studies demonstrated that fucosterol promotes cell viability at concentrations ≤ 100 µg/mL and was also reported to have minimal toxicity on normal human cells (Fernando et al., 2019; Mao et al., 2019). Compared with previous reports,

**Table 5. Fucosterol's oral toxicity profile predictions using ProTox version 3**

Fucosterol oral toxicity prediction	
Predicted LD_{50}	890 mg/kg
Predicted toxicity class	4
Hepatotoxicity	Inactive (0.85)
Carcinogenicity	Inactive (59)
Immunotoxicity	Active (0.99)
Mutagenicity	Inactive (0.96)
Cytotoxicity	Inactive (0.95)

LD_{50}, median lethal dose.

fucosterol showed similar results by exhibiting non-toxic effects on A549 human lung epithelial, dermal fibroblast, and keratinocyte cultures at concentrations lower than 100 µg/mL (Fernando et al., 2019). Moreover, fucosterol was also shown to inhibit cancer cell lines by inducing cell apoptosis and cell cycle arrest, suggesting that fucosterol is a compound capable of promoting cell viability and a concentration-dependent effect on cytotoxicity (Mao et al., 2019).

IL-6 and IL-1β expression on LPS-induced HEK293 cell lines

The inhibitory effect of fucosterol on IL-6 for 24 and 48 h was evaluated through ELISA across five concentrations ranging from 0.1 µg/mL to 62.50 µg/mL. It was compared with the control drug 5 µg/mL DEX, as shown in Fig. 6. DEX was selected as a positive control due to its established anti-inflammatory prop-
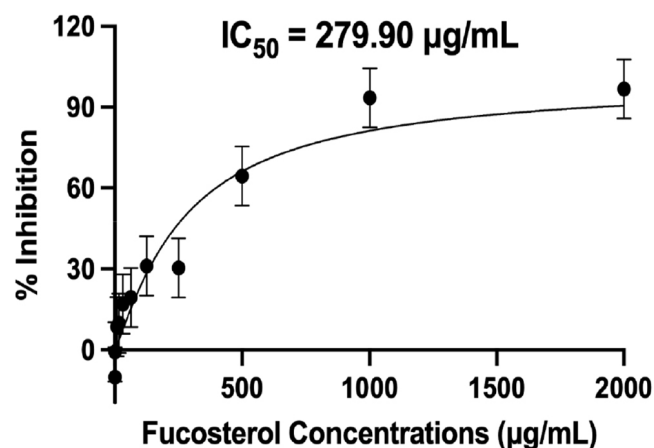
Fig. 5. Fucosterol's IC_{50} on HEK293 cells using MTT assay. IC_{50}, half-maximal inhibitory concentration.
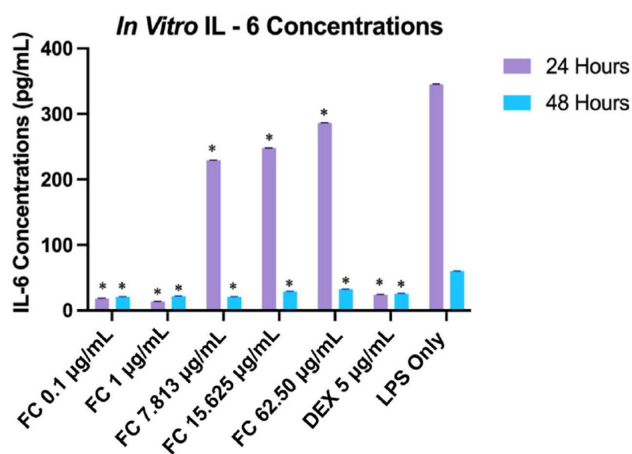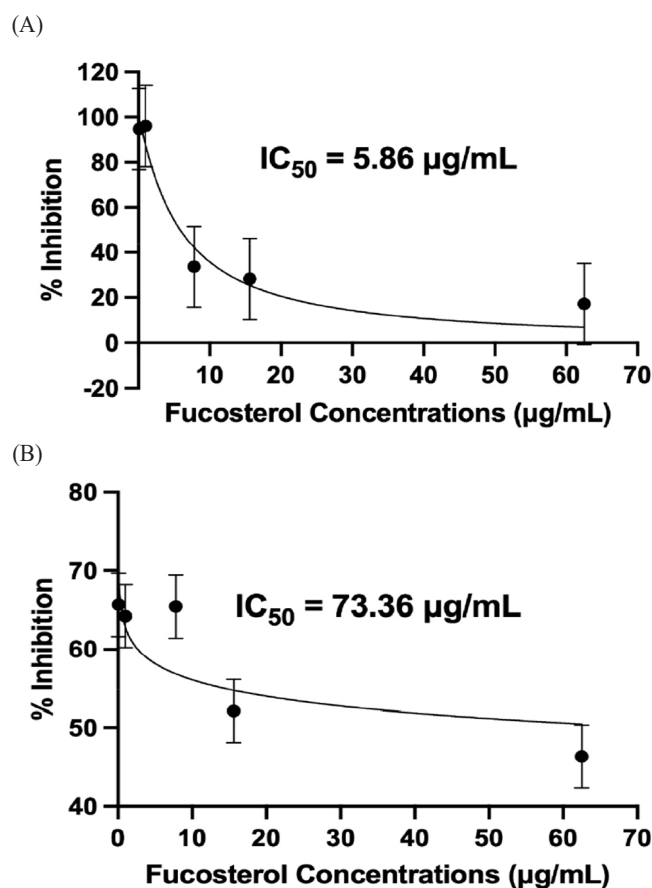
Fig. 6. *In vitro* IL-6 expressions in LPS-induced HEK293 cells at 24 and 48 h using ELISA. Values are presented as concentrations in pg/mL (mean ± SE of 12 replicates). * Indicates significant difference against the LPS only treatment. DEX, dexamethasone; ELISA, Enzyme-Linked Immunosorbent Assay; FC, fucosterol concentration; HEK293, Human Embryonic Kidney; IL, interleukin; LPS, lipopolysaccharide.

erties. As a synthetic glucocorticoid, dexamethasone is known to inhibit the production of pro-inflammatory cytokines, including TNF-α, IL-1β, and IL-6, making it an appropriate reference for assessing anti-inflammatory responses (Patil et al., 2018). This well-established pharmacological profile of dexamethasone allowed for the validation of the assay's sensitivity and provided a reliable benchmark for evaluating the anti-inflammatory activity of the test compounds.
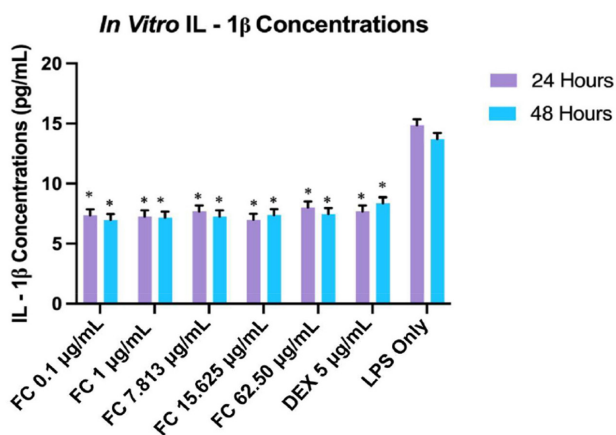
Results indicate that fucosterol exhibited a significantly more substantial inhibitory effect at lower concentrations, with 1 µg/mL showing the least expression after 24 h ($p \le 0.01$). This suggests a biphasic concentration-response relationship, where lower concentrations of fucosterol exhibit beneficial effects, but higher concentrations may lead to reduced efficacy or toxicity (Trela-Makowej et al., 2024). This response has been documented with other phytochemicals like resveratrol and sulforaphane, which exhibit similar biphasic responses (Jodynis-Liebert & Kujawska, 2020). After 48 h, the IL-6 level was significantly reduced, and its expression was substantially higher during the first 24 h, as seen in the LPS-treated cells ($p = 0.03$). Moreover, LPS-treated cells showed a significant difference between 24 and 48 h, indicating that IL-6 expression peaked and was reduced after 48 h ($p \le 0.01$). As seen in Fig. 6, at 24 h, fucosterol concentrations at 0.1 µg/mL and 1 µg/mL showed similar significant inhibitory effects with the positive control DEX when

compared through the expression level of IL-6 ($p = 1.0$ and $p = 0.99$).

This reduction of IL-6 may be related to suppressing the NF-κB pathway, a vital pathway involved in IL-6 transcription, as reported in previous studies (Jayawardena et al., 2020). The biphasic response could be linked to the activation of receptor pathways at lower concentrations and cellular stress responses that may be overwhelmed at higher doses, leading to diminished efficacy or even toxicity (Kageyama & Nemoto, 2022). Fig. 7 shows the IC_{50} values, which were determined to be 5.86 µg/mL (at 24 h) and 73.36 µg/mL (at 48 h), which were significantly different from each other ($p \le 0.05$) and lower than previously reported IC_{50} values, indicating more substantial inhibitory effect under the experimental conditions of this study (Rocha et al., 2022; Wong et al., 2018).
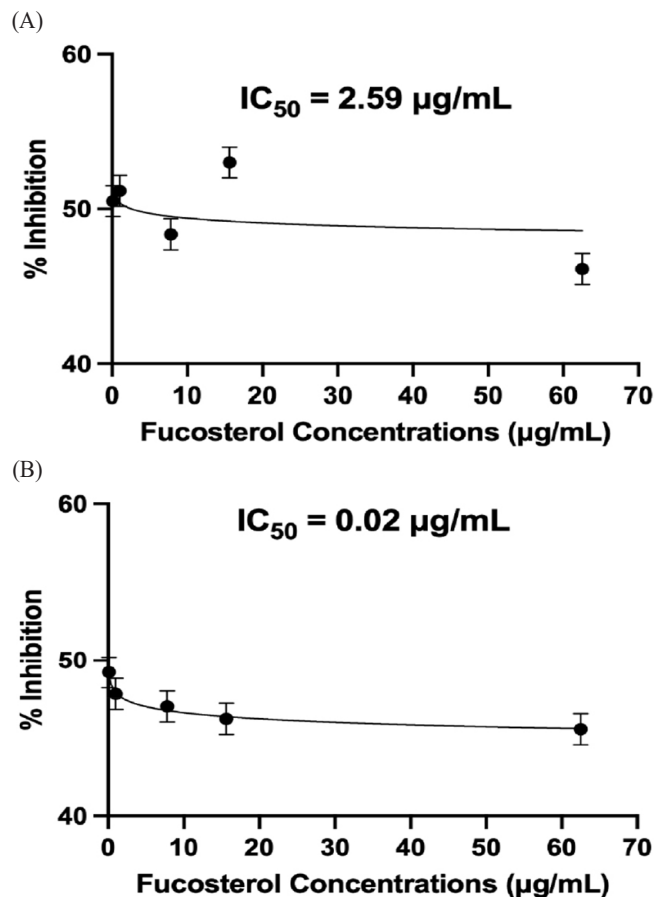
(A)

(B)

Fig. 7. Fucosterol's IC_{50} against IL-6 on LPS-induced HEK293 cells after (A) 24 and (B) 48 h using ELISA. ELISA, Enzyme-Linked Immunosorbent Assay; HEK293, Human Embryonic Kidney; IC_{50}, half-maximal inhibitory concentration; IL, interleukin; LPS, lipopolysaccharide.

Fig. 8. *In vitro* IL-1β expressions in LPS-induced HEK293 cells at 24 and 48 h using ELISA. Values are presented as concentrations in pg/mL (mean ± SE of 12 replicates). [*] Indicates significant difference against the LPS only treatment. DEX, dexamethasone; ELISA, Enzyme-Linked Immunosorbent Assay; FC, fucosterol concentration; HEK293, Human Embryonic Kidney; IL, interleukin; LPS, lipopolysaccharide.

Similarly, fucosterol's inhibitory effect on the expression of IL-1β within 24 and 48 h was evaluated using ELISA (Fig. 8). At 24 h; fucosterol was shown to inhibit IL-1β expression; however, the concentration-response curve showed relatively stable concentrations across various concentrations, suggesting that these concentrations may not significantly alter IL-1β at this period. While the degree of inhibition did not vary significantly among the increasing concentrations, results still highlight a meaningful reduction in IL-1β expression ($p \leq 0.01$). On the other hand, the difference was not significantly different in comparing the IL-1β expression between 24 and 48 h ($p = 0.9861$). Moreover, LPS-treated cells for 24 and 48 h showed significant differences compared to all fucosterol concentrations ($p \leq 0.01$). At the same time, fucosterol did not exhibit a significant difference in its IL-1β expression inhibitory potential than the positive control DEX ($p \geq 0.05$).

Similar to the results of the IL-6 evaluation, the results suggest early saturation of the signaling pathways since lower concentrations are more effective in inhibiting IL-1β. Although no studies have published that fucosterol exhibits this response in IL-1β, prior studies showed that fucosterol can inhibit inflammatory cytokines by modulating the NF-κB and MAPK pathways, thus reducing IL-1β expression (Ghallab et al., 2024; Mo et al., 2018). This suggests that fucosterol's anti-inflammatory effect could be attributed to the modulation of these pathways,

Fig. 9. Fucosterol's IC$_{50}$ against IL-1β on LPS-induced HEK293 cells after (A) 24 and (B) 48 h using ELISA. ELISA, Enzyme-Linked Immunosorbent Assay; HEK293, Human Embryonic Kidney; IC$_{50}$, half-maximal inhibitory concentration; IL, interleukin; LPS, lipopolysaccharide.

although the concentration-response relationship with IL-1β is not as evident as in IL-6. IC$_{50}$ values were computed to be 2.59 μg/mL (at 24 h) and 0.02 μg/mL (at 48 h), as shown in Fig. 9, which were significantly different from each other ($p \leq 0.05$).

The delayed time-dependent effect of fucosterol, as seen by a lower IC$_{50}$ value at 48 h, suggests that its potency and anti-inflammatory activity with IL-1β may involve complex pharmacokinetics and cellular interactions. These findings differ from the results presented in previous studies wherein fucosterol exhibited an immediate concentration-dependent effect on RAW264.7 macrophage cell lines and rat model (Li et al., 2015; Yoo et al., 2012). This discrepancy may be caused by variations in experimental conditions, the cell type, and the inflammatory stimuli used in various studies. One possible explanation for this delayed effect is that fucosterol may require metabolic acti-

vation or accumulation in the cells before exerting its inhibitory effect on the cytokine. Furthermore, the biphasic response indicates that fucosterol may act on several pathways or work indirectly by modifying the transcription factors generating these cytokines in HEK293 cells (Hayakawa & Qiu, 2010).

Furthermore, these findings highlight the potential of fucosterol as a promising anti-inflammatory agent, even at lower concentrations, which could have significant implications for therapeutic applications. Effective lower concentrations may reduce the risk of cytotoxicity and side effects, making fucosterol a favorable candidate for drug development (Meinita et al., 2021). However, further investigations are necessary to elucidate the molecular mechanisms underlying its time-dependent activity and biphasic response. Future research should identify specific signaling pathways, receptor interactions, and possible metabolic modifications contributing to the observed effects to optimize dosing strategies for clinical applications.

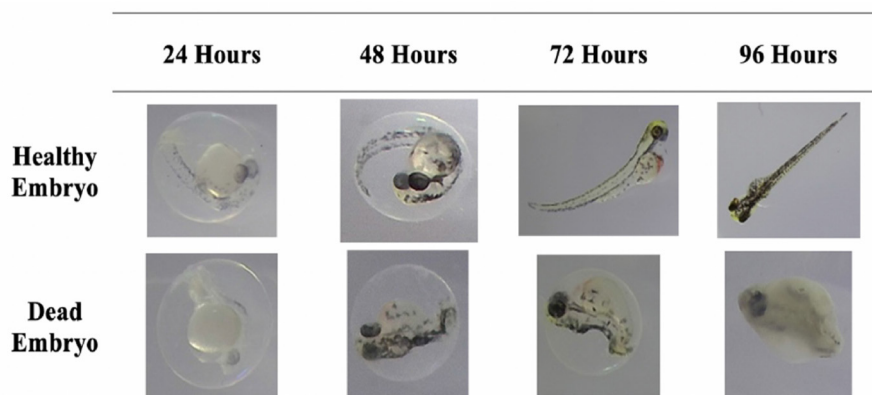### Fucosterol's acute toxicity effect on zebrafish embryos

A significant lethality rate was observed at higher concentrations of fucosterol in the acute toxicity assay using zebrafish embryos ($p \leq 0.01$). Fig. 10 shows the comparison between the development of zebrafish embryos treated with ≤ 100 μg/mL (healthy) and > 100 μg/mL (dead) of fucosterol.

As seen in the figure, the healthy embryo could fully develop the somite or the backbone of the fish at 48 h and exhibit a heartbeat, marked by the reddish part near the head of the fish, at 72 h. These features were lacking in the embryo treated with higher concentrations of fucosterol, which can be considered dead already due to lack of somite formation at 48 h

and the coagulation of the whole body after 96 h. At 96 h, a healthy embryo could fully develop its tail, show a heartbeat, and exhibit locomotion, which signifies survival and continuous development. After 48 h, concentrations above 100 μg/mL already showed 50% lethality in the zebrafish embryos, indicating toxicity. At 96 h, 13% mortality was observed at 100 μg/mL, which falls under the acceptable limit to be considered non-toxic. The significant difference ($p \leq 0.01$) in lethality rates between various concentrations highlights fucosterol's concentration-dependent response to fucosterol in the model. Moreover, 3,4-dichloroaniline, an environmental pollutant known to cause oxidative stress, was used as the positive control based on OECD guidelines which resulted in a 90% lethality rate after the 96-hour testing period (OECD, 2013). LC_{50} was determined to be 173.60 μg/mL, which supports the result of the study that higher concentrations have a more substantial lethal effect, as shown in Fig. 11. Since concentrations ≤ 100 μg/mL were considered to be non-toxic, concentrations lower than this were used for subsequent assays to ensure the safety of the embryos during the testing process.

IL-6 and IL-1β expression on LPS-induced zebrafish embryos

Various concentrations of fucosterol (6.25 μg/mL to 100 μg/mL) and the control drug DEX were used to evaluate IL-6 and IL-1β expression on zebrafish embryos through ELISA. For both cytokines, a concentration-dependent reduction was observed with increasing inhibition at higher concentrations of fucosterol. For IL-6, both 24 and 48-hour observations consistently showed a significant reduction in IL-6, suggesting its effective role in modulating the inflammatory cytokine ($p \leq 0.01$; Fig. 12).
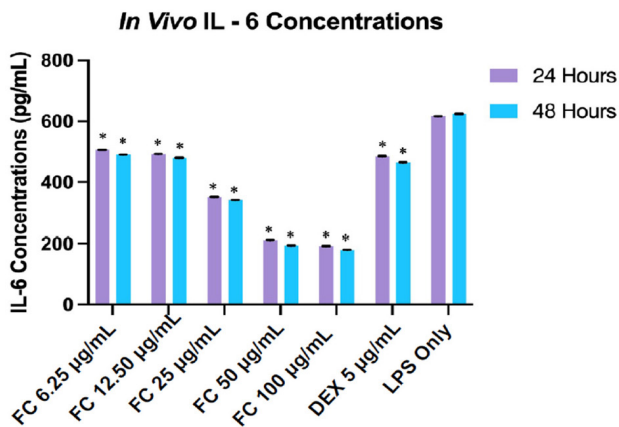

Fig. 10. Healthy vs dead zebrafish embryo development during acute toxicity testing of fucosterol.
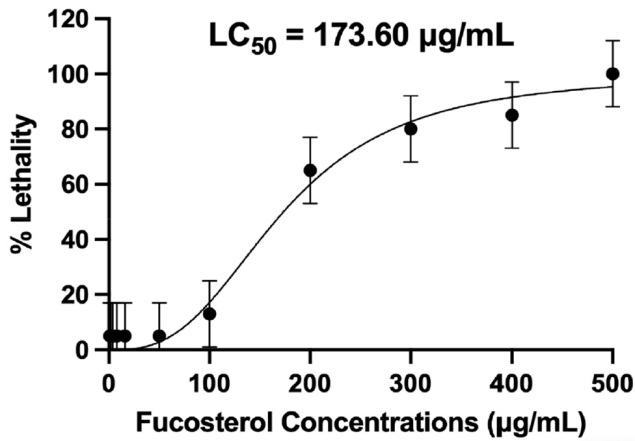
Fig. 11. Fucosterol's LC$_{50}$ on zebrafish embryo through fish embryo acute toxicity assay. LC$_{50}$, medial lethal concentration.
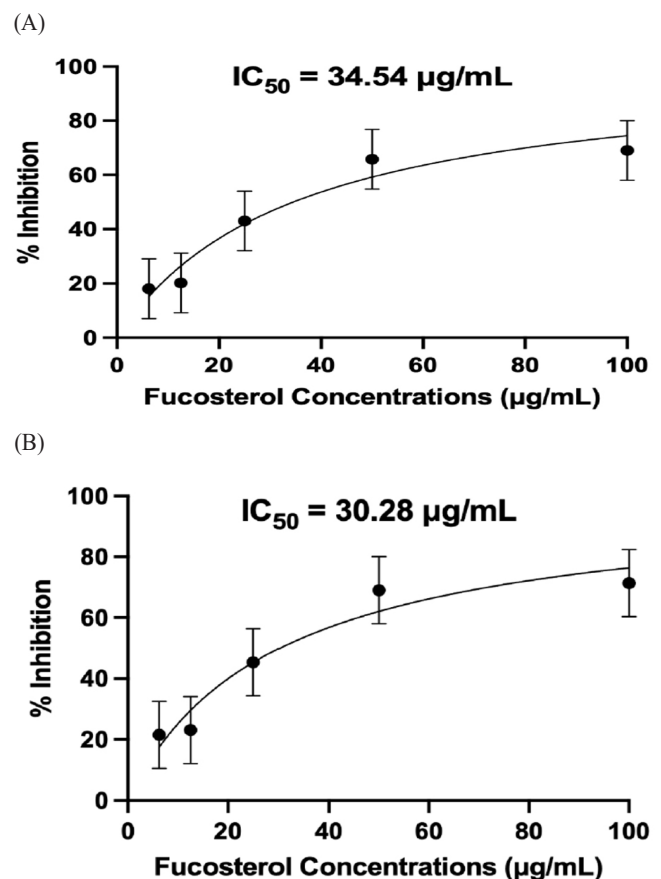

Fig. 12 . *In vivo* **IL-6 expressions in LPS-treated zebrafish embryos at 24 and 48 h using ELISA.** Values are presented as concentrations in pg/mL (mean ± SE of 6 replicates). * Indicates significant difference against the LPS only treatment. DEX, dexamethasone; ELISA, Enzyme-Linked Immunosorbent Assay; FC, fucosterol concentration; IL, interleukin; LPS, lipopolysaccharide.

At 50 µg/mL and 100 µg/mL, fucosterol exhibited better inhibition than DEX, indicating that fucosterol may be more active than the standard anti-inflammatory treatment at these concentrations ($p \leq 0.01$). Moreover, at 12.50 µg/mL, fucosterol exhibited a similar inhibitory effect to the control drug DEX ($p = 0.826$). The results support a concentration-dependent relationship, indicating that fucosterol's efficacy increases as the concentration increases. However, this effect reached a plateau at higher concentrations, likely due to receptor saturation, which needs further evaluation. The findings for IL-6 inhibi-

tion in this study align with previous experiments examining the anti-inflammatory properties of fucosterol in other animal models where IL-6 was reduced in mice with liver injury and skeletal muscle atrophy by modulating the Akt/mTOR/FoxO3α pathway (Hwang et al., 2024; Mo et al., 2018). Moreover, previous studies also highlighted fucosterol's potential to suppress NF-κB and MAPK signaling pathways, which play key roles in cytokine production, and further validate the results of this study (Meinita et al., 2021). IC$_{50}$ values for IL-6 were computed to be 34.54 µg/mL (at 24 h) and 30.28 µg/mL (at 48 h), with no significant difference from the two incubation periods ($p = 0.33$; Fig. 13).

Fucosterol's effect on the expression of IL-1β was also revealed to be concentration-dependent where higher concentrations, like 50 µg/mL and 100 µg/mL, significantly suppressed IL-1β levels, comparable to or even surpassing the effect of DEX

(A)

(B)

Fig. 13. Fucosterol's IC$_{50}$ against IL-6 on LPS-induced zebrafish embryos after (A) 24 and (B) 48 h using ELISA. ELISA, Enzyme-Linked Immunosorbent Assay; IC$_{50}$, half-maximal inhibitory concentration; IL, interleukin; LPS, lipopolysaccharide.
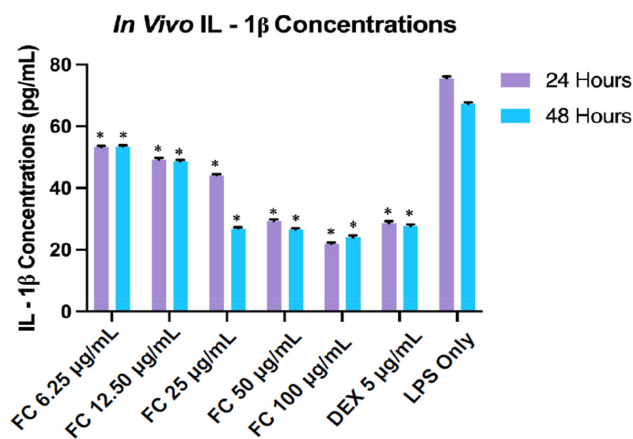
Fig. 14. *In vivo* **IL-1β expressions in LPS-treated zebrafish embryos at 24 and 48 h using ELISA.** Values are presented as concentrations in pg/mL (mean ± SE of 6 replicates). * Indicates significant difference against the LPS only treatment. DEX, dexamethasone; ELISA, Enzyme-Linked Immunosorbent Assay; FC, fucosterol concentration; IL, interleukin; LPS, lipopolysaccharide.

($p \leq 0.01$; Fig. 14).

In addition, fucosterol concentration of 50 μg/mL showed no significant difference compared to the effects of the control drug DEX ($p = 0.998$). Moreover, IL-1β levels in LPS-treated embryos for 24 and 48 h showed significant differences compared to all fucosterol and DEX treatments ($p \leq 0.01$). Interestingly, IL-1β expression was slightly lower after 48 h, suggesting either an adaptive immune response or prolonged efficacy of fucosterol over time. Similarly, IC$_{50}$ values for IL-1β for 24 and 48 h were found to have no significant difference and were determined to be 29.39 μg/mL and 29.61 μg/mL, respectively ($p = 0.38$; Fig. 15).

A comparison between the IC$_{50}$ values from the *in vitro* assay revealed a notable discrepancy, as fucosterol appeared to be more effective at lower concentrations in cell line assays and was found to have a significant difference between the IC$_{50}$ values from 24 and 48 h incubation. This difference likely results from fucosterol directly interacting with isolated cells in cell line assays, thus achieving maximal efficacy at lower concentrations. In contrast, in *an in vivo* setting, fucosterol must be absorbed first and metabolized, requiring higher concentrations to elicit beneficial effects and achieve bioavailability. The findings of the *in vivo* studies support previously reported data that fucosterol can reduce IL-1β levels in a liver injury model through mod-
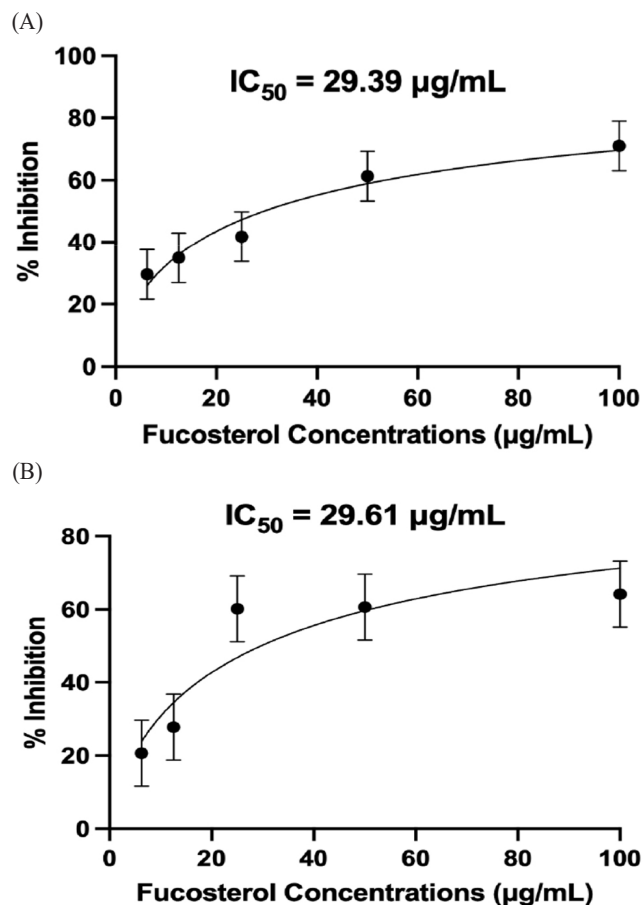
Fig. 15. Fucosterol's IC$_{50}$ against IL-1β on LPS-induced zebrafish embryos after (A) 24 and (B) 48 h using ELISA. ELISA, Enzyme-Linked Immunosorbent Assay; IC$_{50}$, half-maximal inhibitory concentration; IL, interleukin; LPS, lipopolysaccharide.

ulation of the P38 MAPK and NF-κB pathways (Hwang et al., 2024; Mo et al., 2018). Moreover, fucosterol has also been found to possess antioxidant properties, which may contribute to the reduction of oxidative stress, which is vital in the synthesis of IL-6 (Meinita et al., 2021). Further studies are needed to explore the broader applications of fucosterol, especially in clinical settings, and evaluate its efficacy and safety in human patients. The consistency of results across various studies shows that fucosterol can elicit an anti-inflammatory effect due to its ability to modulate the production of IL-6 and IL-1β by inhibiting the NF-κB pathway. The potential for fucosterol to be developed as a pharmaceutical product is underscored by its concentration-dependent effects and ability to modulate critical inflammatory pathways. Thus, further studies, including pre-formulation studies and comprehensive mechanistic evaluations, will

Fisheries and Aquatic Sciences

help establish the compound's potential as a pharmacological product.

Conclusions

The study demonstrated fucosterol's potential as an anti-inflammatory agent based on insights from reverse molecular docking, *in vitro*, and *in vivo* evaluations. Molecular docking revealed strong binding affinities with pro-inflammatory proteins IL-6 and IL-1β, with potential inhibitory effects validated through ELISA using LPS-induced HEK293 cells and zebrafish embryo models. Fucosterol also showed favorable drug-likeness profiles. However concerns regarding its water solubility limit its clinical application, emphasizing the need for advanced delivery systems to enhance its bioavailability and reduce toxicity. Recommendations for future research include exploring the molecular mechanism of IL-6 and IL-1β inhibition and performing long-term toxicity studies by validating in higher animal models.

Availability of data and materials
Upon reasonable request, the datasets of this study can be available from the corresponding author.

Ethics approval and consent to participate
This research has been approved by the Institutional Animal Care and Use Committee (IACUC) of the University of Santo Tomas, Manila, Philippines (RC2024-320907) and was cleared by the Philippine Bureau of Animal Industry, Manila, Philippines (AR-2024-0512).

ORCID
Rickson Gaspe   https://orcid.org/0009-0004-4044-237X
Junie Billones   https://orcid.org/0000-0001-6257-7292
Agnes Llamasares-Castillo
   https://orcid.org/0000-0002-6167-3431

References

Abdul QA, Choi RJ, Jung HA, Choi JS. Health benefit of fucosterol from marine algae: a review. J Sci Food Agric. 2016;96:1856-66.

Agu PC, Afiukwa CA, Orji OU, Ezeh EM, Ofoke IH, Ogbu CO, et al. Molecular docking as a tool for the discovery of molecular targets of nutraceuticals in diseases management. Sci Rep. 2023;13:13398.

Alos HC, Billones JB, Vasquez RD, Castillo AL. Antiangiogenesis potential of alpinumisoflavone as an inhibitor of matrix metalloproteinase-9 (MMP-9) and vascular endothelial growth factor receptor-2 (VEGFR-2). Curr Enzyme Inhib. 2020;15:159-78.

Aventurado CA, Billones JB, Vasquez RD, Castillo AL. In ovo and in silico evaluation of the anti-angiogenic potential of syringin. Drug Des Dev Ther. 2020;14:5189-204.

Aykul S, Martinez-Hackert E. Determination of half-maximal inhibitory concentration using biosensor-based protein interaction analysis. Anal Biochem. 2016;508:97-103.

Bell EW, Zhang Y. DockRMSD: an open-source tool for atom mapping and RMSD calculation of symmetric molecules through graph isomorphism. J Cheminform. 2019;11:40.

Bin XN, Gao YB, Pan M, Lian ZL, Cheng YZ, Wu JQ, et al. Anti-inflammatory effects of 6S-5-methyltetrahydrofolate-calcium on RAW264.7 cells and zebrafish. Life Sci. 2023;327:121839.

Chen L, Deng H, Cui H, Fang J, Zuo Z, Deng J, et al. Inflammatory responses and inflammation-associated diseases in organs. Oncotarget. 2018;9:7204-18.

Erukainure OL, Narainpersad N, Singh M, Olakunle S, Islam MS. *Clerodendrum volubile* inhibits key enzymes linked to type 2 diabetes but induces cytotoxicity in human embryonic kidney (HEK293) cells via exacerbated oxidative stress and proinflammation. Biomed Pharmacother. 2018;106:1144-52.

Fernando IPS, Jayawardena TU, Kim HS, Lee WW, Vaas APJP, De Silva HIC, et al. Beijing urban particulate matter-induced injury and inflammation in human lung epithelial cells and the protective effects of fucosterol from *Sargassum binderi* (*Sonder ex J. Agardh*). Environ Res. 2019;172:150-8.

Franceschi C, Campisi J. Chronic inflammation (inflammaging) and its potential contribution to age-associated diseases. J Gerontol Ser A. 2014;69:S4-9.

Gabay C. Interleukin-6 and chronic inflammation. Arthritis Res Ther. 2006;8:S3.

Germolec DR, Shipkowski KA, Frawley RP, Evans E. Markers of inflammation. Methods Mol Biol. 2018;1803:57-79.

Gerriets V, Goyal A, Khaddour K. Tumor necrosis factor inhibitors. Petersburg, FL: StatPearls Publishing; 2023.

Ghallab DS, Ibrahim RS, Mohyeldin MM, Shawky E. Marine algae: a treasure trove of bioactive anti-inflammatory compounds. Mar Pollut Bull. 2024;199:116023.

Hayakawa K, Qiu J, Lo EH. Biphasic actions of HMGB1 signaling in inflammation and recovery after stroke. Ann N Y Acad Sci. 2010;1207:50-7.

Hwang J, Kim MB, Lee S, Hwang JK. Fucosterol, a phytosterol of marine algae, attenuates immobilization-induced skeletal muscle atrophy in C57BL/6J mice. Mar Drugs. 2024;22:557.

Jang H, Lee J, Park YK, Lee JY. Exploring the health benefits and concerns of brown seaweed consumption: a comprehensive review of bioactive compounds in brown seaweed and its potential therapeutic effects. J Agric Food Res. 2024;17:101215.

Javadi S, Moradhaseli S, Mirakabadi AZ, Lotfi M, Bidoki K. Assessment of apoptotic impact of ICD-85 in A549 cancer cells & HEK293 normal cells. Gene Rep. 2020;20:100746.

Jayawardena TU, Sanjeewa KKA, Lee HG, Nagahawatta DP, Yang HW, Kang MC, et al. Particulate matter-induced inflammation/oxidative stress in macrophages: fucosterol from *Padina boryana* as a potent protector, activated via NF-κB/MAPK pathways and Nrf2/HO-1 involvement. Mar Drugs. 2020;18:628.

Jodynis-Liebert J, Kujawska M. Biphasic dose-response induced by phytochemicals: experimental evidence. J Clin Med. 2020;9:718.

Kageyama K, Nemoto T. Molecular mechanisms underlying stress response and resilience. Int J Mol Sci. 2022;23:9007.

Kazmi SR, Jun R, Yu MS, Jung C, Na D. *In silico* approaches and tools for the prediction of drug metabolism and fate: a review. Comput Biol Med. 2019;106:54-64.

Li Y, Li X, Liu G, Sun R, Wang L, Wang J, et al. Fucosterol attenuates lipopolysaccharide-induced acute lung injury in mice. J Surg Res. 2015;195:515-21.

Mao Z, Shen X, Dong P, Liu G, Pan S, Sun X, et al. Fucosterol exerts antiproliferative effects on human lung cancer cells by inducing apoptosis, cell cycle arrest and targeting of Raf/MEK/ERK signalling pathway. Phytomedicine. 2019;61:152809.

Meinita MDN, Harwanto D, Tirtawijaya G, Negara BFSP, Sohn JH, Kim JS, Choi JS. Fucosterol of marine macroalgae: Bioactivity, safety and toxicity on organism. Mar Drugs. 2021;19(10):545. https://doi.org/10.3390/md19100545

Mo W, Wang C, Li J, Chen K, Xia Y, Li S, et al. Fucosterol protects against concanavalin A-induced acute liver injury: focus on P38 MAPK/NF-κB pathway activity. Gastroenterol Res Pract. 2018;2018:1-13.

Nadri MH, Salim Y, Basar N, Yahya A, Zulkifli RM. Antioxidant activities and tyrosinase inhibition effects of *Phaleria macrocarpa* extracts. Afr J Tradit Complement Altern Med. 2014;11:107-11.

Novoa B, Figueras A. Zebrafish: model for the study of inflammation and the innate immune response to infectious diseases. Adv Exp Med Biol. 2011;946:253-75.

Organization for Economic Cooperation and Development (OECD). Test no. 236: fish embryo acute toxicity (FET) test. Paris: OECD; 2013. Report no.: OECD guidelines for the testing of chemicals, section 2.

Ornos ED, Murillo KJ, Ong JP. Liver diseases: perspective from the Philippines. Ann Hepatol. 2023;28:101085.

Patil RH, Naveen Kumar M, Kiran Kumar KM, Nagesh R, Kavya K, Babu RL, et al. Dexamethasone inhibits inflammatory response via down regulation of AP-1 transcription factor in human lung epithelial cells. Gene. 2018;645:85-94.

Philippine Statistics Authority (PSA). 2022 Causes of deaths in the Philippines (preliminary as of 28 February 2023). [Internet]. PSA. 2023 [cited 2025 Jan 2]. https://psa.gov.ph/content/2022-causes-deaths-philippines-preliminary-28-february-2023

Pirlamarla P, Bond RM. FDA labeling of NSAIDs: review of nonsteroidal anti-inflammatory drugs in cardiovascular disease. Trends Cardiovasc Med. 2016;26:675-80.

Raghubeer S, Nagiah S, Chuturgoon AA. Acute ochratoxin A exposure induces inflammation and apoptosis in human embryonic kidney (HEK293) cells. Toxicon. 2017;137:48-53.

Rahman MA, Dash R, Sohag AAM, Alam M, Rhim H, Ha H, et al. Prospects of marine sterols against pathobiology of Alzheimer's disease: pharmacological insights and technological advances. Mar Drugs. 2021;19:167.

Rocha DHA, Pinto DCGA, Silva AMS. Macroalgae specialized metabolites: evidence for their anti-inflammatory health benefits. Mar Drugs. 2022;20:789.

Sun Z, Antar Aziz Mohamed M, Park SY, Yi TH. Fucosterol protects cobalt chloride induced inflammation by the inhibition of hypoxia-inducible factor through PI3K/Akt pathway. Int Immunopharmacol. 2015;29:642-7.

Tan E, Chin CSH, Lim ZFS, Ng SK. HEK293 cell line as a platform to produce recombinant proteins and viral vectors. Front Bioeng Biotechnol. 2021;9:796991.

Tran QH, Nguyen QT, Vo NQH, Mai TT, Tran TTN, Tran TD, et al. Structure-based 3D-pharmacophore modeling to discover novel interleukin 6 inhibitors: an *in silico* screening, molecular dynamics simulations and binding free energy calculations. PLOS ONE. 2022;17:e0266632.

Trela-Makowej A, Orzechowska A, Szymańska R. *Less is more*: the hormetic effect of titanium dioxide nanoparticles on plants. Sci Total Environ. 2024;910:168669.

Turner MD, Nedjai B, Hurst T, Pennington DJ. Cytokines and chemokines: at the crossroads of cell signalling and inflammatory disease. Biochim Biophys Acta Mol Cell Res. 2014;1843:2563-82.

Wang L, Je JG, Huang C, Oh JY, Fu X, Wang K, et al. Anti-inflammatory effect of sulfated polysaccharides isolated from *Codium fragile in vitro* in RAW 264.7 macrophages and *in vivo* in zebrafish. Mar Drugs. 2022;20:391.

Wang Y, Tian J, Shi F, Li X, Hu Z, Chu J. Protective effect of surfactin on copper sulfate-induced inflammation, oxidative stress, and hepatic injury in zebrafish. Microbiol Immunol. 2021;65:410-21.

Wong CH, Gan SY, Tan SC, Gany SA, Ying T, Gray AI, et al. Fucosterol inhibits the cholinesterase activities and reduces the release of pro-inflammatory mediators in lipopolysaccharide and amyloid-induced microglial cells. J Appl Phycol. 2018;30:3261-70.

Yadav A, Mandal MK, Dubey KK. *In vitro* cytotoxicity study of cyclophosphamide, etoposide and paclitaxel on monocyte macrophage cell line raw 264.7. Indian J Microbiol. 2020;60:511-7.

Yatoo MI, Gopalakrishnan A, Saxena A, Parray OR, Tufani NA, Chakraborty S, et al. Anti-inflammatory drugs and herbs with special emphasis on herbal medicines for countering inflammatory diseases and disorders - a review. Recent Pat Inflamm Allergy Drug Discov. 2018;12:39-58.

Yang LL, Wang GQ, Yang LM, Huang ZB, Zhang WQ, Yu LZ. Endotoxin molecule lipopolysaccharide-induced zebrafish inflammation model: a novel screening method for anti-inflammatory drugs. Molecules. 2014;19:2390-409.

Yoo MS, Shin JS, Choi HE, Cho YW, Bang MH, Baek NI, et al. Fucosterol isolated from *Undaria pinnatifida* inhibits lipopolysaccharide-induced production of nitric oxide and pro-inflammatory cytokines via the inactivation of nuclear factor-κB and p38 mitogen-activated protein kinase in RAW264.7 macrophages. Food Chem. 2012;135:967-75.

Yoojam S, Ontawong A, Lailerd N, Mengamphan K, Amornlerdpison D. The enhancing immune response and anti-inflammatory effects of *Caulerpa lentillifera* extract in RAW 264.7 cells. Molecules. 2021;26:5734.